Diagnostic Usefulness of Combination of Diffusion-weighted Imaging and T2WI, Including Apparent Diffusion Coefficient in Breast Lesions: Assessment of Histologic Grade

Keum Won Kim, MD, PhD, Cherie M. Kuzmiak, DO, Young Joong Kim, MD, Jae Young Seo, MD, Hae Kyoung Jung, MD, Mu-Sik Lee, MD, PhD

Purpose: This study aimed to compare the diagnostic values of a combination of diffusion-weighted imaging and T2-weighted imaging (DWI-T2WI) with dynamic contrast-enhanced magnetic resonance imaging (DCE-MRI), and to evaluate the correlation of DWI with the histologic grade in breast cancer.

Materials and Methods: This study evaluated a total of 169 breast lesions from 136 patients who underwent both DCE-MRI and DWI (b value, 1000s/mm^2). Morphologic and kinetic analyses for DCE-MRI were classified according to the Breast Imaging-Reporting and Data System. For the DWI-T2WI set, a DWI-T2WI score for lesion characterization that compared signal intensity of DWI and T2WI (benign: DWI-T2WI score of 1, 2; malignant: DWI-T2WI score of 3, 4, 5) was used. The diagnostic values of DCE-MRI, DWI-T2WI set, and combined assessment of DCE and DWI-T2WI were calculated.

Results: Of 169 breast lesions, 48 were benign and 121 were malignant (89 invasive ductal carcinoma, 24 ductal carcinoma in situ, 4 invasive lobular carcinoma, 4 mucinous carcinoma). The mean apparent diffusion coefficient (ADC) of invasive ductal carcinoma ($0.92 \pm 0.19 \times 10^{-3}$ mm^2/s) and ductal carcinoma in situ ($1.11 \pm 0.13 \times 10^{-3}$ mm^2/s) was significantly lower than the value seen in benign lesions ($1.36 \pm 0.22 \times 10^{-3}$ mm^2/s). The specificity, positive predictive value (PPV), and accuracy of DWI-T2WI set and combined assessment of DCE and DWI-T2WI (specificity, 87.5% and 91.7%; PPV, 94.3% and 96.2%; accuracy, Az = 0.876 and 0.922) were significantly higher than those of the DCE-MRI (specificity, 45.8%; PPV, 81.7%; accuracy, Az = 0.854; $P < .05$). A low ADC value and the presence of rim enhancement were associated with a higher histologic grade cancer ($P < .05$).

Conclusion: Combining DWI, T2WI, and ADC values provides increased accuracy for differentiation between benign and malignant lesions, compared with DCE-MRI. A lower ADC value was associated with a higher histologic grade cancer.

Key Words: Breast cancer; magnetic resonance imaging; diffusion-weighted imaging; apparent diffusion coefficient.

INTRODUCTION

Diffusion-weighted imaging (DWI) is currently being evaluated to increase the specificity of breast magnetic resonance imaging (MRI) (1–3). DWI is a noninvasive technique that uses the biological characteristics of Brownian movement of protons in water. High signal intensity (SI) on DWI and a low apparent diffusion coefficient (ADC) value are correlated with highly cellular tissue and decreased movement of molecules (4–7). When DWI is used, malignant breast lesions have higher SI than with T2-weighted imaging (T2WI) fast spin echo (FSE) MRI, and malignant breast lesions have low ADC values. Malignant breast

Acad Radiol 2018; 25:643–652

From the Department of Radiology, Konyang University Hospital, College of Medicine, Myunggok Medical Research Center, Daejeon, Republic of Korea (K.W.K., Y.J.K., J.Y.S.); Department of Radiology, University of North Carolina, CB #7510, Physicians' Office Building, Rm #118, 170 Manning Drive, Chapel Hill, NC 27599 (C.M.K.); Department of Radiology, CHA Bundang Medical Center, CHA University, Seongnam (H.K.J.); Department of Preventive Medicine, Konyang University, College of Medicine, Daejeon, Republic of Korea (M.-S.L.). Received August 31, 2017; revised October 31, 2017; accepted November 10, 2017. **Address correspondence to:** C.M.K. e-mail: cherie_kuzmiak@med.unc.edu

https://doi.org/10.1016/j.acra.2017.11.011

lesions display lower SI on T2WI than benign lesions because of shorter T2 relaxation time (8). The high cellularity of cancer cell caused the restriction of Brownian motion in extracellular water molecules around cancer cells. In contrast, fluid in cysts consists of free water molecules and a higher ADC (9,10).

Multiple studies have evaluated DWI and ADC value for breast tumor and evaluated the diagnostic value of combined dynamic contrast-enhanced (DCE) MRI and DWI for breast cancer detection (11–15). The detectability on DWI was higher than T1WI or T2WI for breast tumor, and the mean ADC value of invasive ductal carcinoma (IDC) and ductal carcinoma in situ (DCIS) were lower than benign breast lesions. Kul et al. revealed (11) the combination of DWI and DCE-MRI has the potential to increase the specificity of breast MRI. Another study reported that combined DCE-MRI and DWI had superior diagnostic accuracy than either DCE-MRI or DWI alone for the diagnosis of breast cancer (15). However, those studies did not compare each SI between DWI and T2WI for characterization of the lesion. In addition, those studies did not compare the accuracy of DWI-T2WI combination with that of DCE-MRI. In those studies, T2WI and DCE-MRI were used as pilot images for localizing the lesion. Thus, the purpose of our study is to compare the diagnostic values of a combination of DWI and T2WI with DCE-MRI, and to investigate the correlation of DWI, including ADC value, with the histologic grade in breast cancer lesions.

MATERIALS AND METHODS

Our institutional review board approved the study and waived patient informed consent because of the retrospective design. A total of 205 women with 230 breast lesions were initially included in this study. All included subjects underwent breast MRI between January 2011 and December 2015. There were 69 subjects with 61 lesions who did not have follow-up or histopathologic confirmation and were excluded from the study. Our final study population consisted of 136 women with 169 lesions (mean age, 48.6 years; range, 31–70 years). The diagnosis for all 169 lesions was confirmed by pathology. A total of 130 lesions (77%) were confirmed using surgically excised specimens: 45 (35%) modified radical mastectomy; 67 (51%) lumpectomy; 18 (14%) excisional biopsy. A total of 39 lesions (23%) were confirmed from a core needle biopsy specimen.

MRI Protocol

MRI examinations were performed using a 3.0 Tesla MRI system (Achieva 3.0T TX, Philips Medical Systems, Best, the Netherlands) and a breast coil (Philips, Sense breast coil 4ch 3.0T, Best, the Netherlands). To minimize the respiratory-motion artifact, the subjects were placed in the prone position and the imaging was performed. The protocols of each sequence of breast MRI are summarized in Table 1. This final scan was obtained before a rapid bolus injection of 0.1 mmol/kg of gadobutrol (Gadovist, Bayer Schering Pharma AG, Berlin, Germany). Scanning was repeated 1, 2, 3, 4, 5, 6, and 7 minutes after contrast administration. Subtraction images were obtained by subtracting the precontrast images from the postcontrast images on a pixel-by-pixel basis.

DWI Acquisition and ADC Analysis

The ADC was calculated according to the equation: ADC = (1/b2 − b1) ln (S2/S1), where S1 and S2 were the SIs in the regions of interest (ROIs) obtained using different gradient factors (b values of 0 and 1000 s/mm^2). For measuring the ADC value, two breast imaging radiologists, who were blinded to the results of the study, manually placed an ROI. When compared with DCE-MRI, the enhancing solid portion of the tumor was used to site the ADC measurement. The same radiologists reviewed images in consensus. An ROI at the corresponding location was manually defined on averaged DWI to include the area of hyperintensity. The

TABLE 1. Protocols of Each Sequence of Breast MRI

	Fat-suppressed Turbo Spin-echo (TSE-FS) T2WI	Postcontrast T1WI Fast Field Echo (T1WI-FFE)	DW Single-shot Echo-planar Imaging with Sensitivity Encoding (SENSE)
TR/TE	4375/70	4.4/1.6	1835/57
Flip angle	90°	10°	90°
Slices	30	270	30
Field of view	350 × 350 mm	340 × 340 mm	350 × 350 mm
Matrix	528 × 512	512 × 510	116 × 115
Number of excitation (NEX)	1.0	1.0	2.0
SENSE	1.5	2.0	0
Section thickness	4 mm	1.5 mm	4 mm
Intersection gap	0	0	0
Acquisition time	4 min	8 min	3 min
b Value			0 and 1000 s/mm^2

DW, diffusion-weighted; MRI, magnetic resonance imaging; TR/TE, repetition time/echo time; T1WI, T1-weighted imaging; T2WI, T2-weighted imaging.

TABLE 2. Reader DWI-T2WI Score with Corresponding Probability of Malignancy and DWI Findings for Lesion Characterization

DWI-T2WI score 1	Definitely benign	T2 high SI/DWI low SI
DWI-T2WI score 2	Probably benign	T2 high SI/DWI intermediate SI
DWI-T2WI score 3	Possibly malignant	T2 high SI/DWI high SI
DWI-T2WI score 4	Probably malignant	T2 intermediate SI/DWI high SI
DWI-T2WI score 5	Definitely malignant	T2 intermediate or low SI/DWI very high SI

DWI-T2WI, diffusion-weighted imaging and T2-weighted imaging; SI, signal intensity

ADC values were automatically measured by drawing the ROIs. The two measurements were averaged and used as the ADC value.

Reader Study Analysis

The images were divided into two sets. DCE-MRI set consisted of pre- and postcontrast dynamic-enhanced T1 fast field echo images. DWI-T2WI set consisted of DWI and T2WI fat-suppressed turbo-spin echo and DWI using b values of 1000 s/mm^2. Two radiologists trained in breast imaging individually interpreted the different images that marked the images without being provided any clinical or pathologic information, with consensus.

In the DCE-MRI set, magnetic resonance images were interpreted according to the Breast Imaging-Reporting and Data System (BI-RADS) criteria. The lesions were assessed with one of the five BI-RADS categories. When there was no mass or any contrast enhancement, the study was categorized as BI-RADS 1 (negative). A focal mass with round, oval shape; smooth margin; non-enhancing internal septations; and a persistent type of enhancement (kinetic curve 1) was categorized as BI-RADS 2 (benign). Focal masses with round, oval shape; smooth margin; persistent type of enhancement (kinetic curve 1); and asymmetric non-mass enhancement of focal or regional distribution were categorized as BI-RADS 3 (probably benign). A mass with irregular shape; irregular or spiculated margin; heterogeneous or rim enhancement; non-mass lesions with clumped and clustered ring enhancement at ductal or segmental distribution; and plateau or wash-out time course (kinetic curve 2 or 3) was categorized as BI-RADS 4 (suspicious). A mass or non-mass lesion with suspicious morphology; more than 90% wash-in rate; and wash-out time course (kinetic curve 3) was categorized as BI-RADS 5 (highly suggestive of malignancy). In the DWI-T2WI set, DWI-T2WI scores were categorized from 1 to 5, by comparing the SI of DWI and T2WI. Further, the ADC value of each lesion was calculated using the b value of 1000 s/mm^2. The readers used the DWI-T2WI score for lesion characterization into five grades: high SI on T2WI and low SI on DWI was categorized as DWI-T2WI score 1 (definitely benign); high SI on T2WI and intermediate SI on DWI was categorized as DWI-T2WI score 2 (probably benign); high SI on T2WI and high SI on DWI was categorized as DWI-T2WI score 3 (possibly malignant); intermediate SI on T2WI and high SI on DWI was categorized as DWI-T2WI score 4 (probably malignant); and intermediate or low SI on T2WI and very high SI on DWI was categorized as DWI-T2WI score 5 (definitely malignant) (Table 2, Fig 1). The value of combined assessment of DCE and DWI-T2WI was designed as the sum of the BI-RADS and the DWI-T2WI score. For the combined assessment of MRI, sum of the BI-RADS and DWI-T2WI score of 6 or greater was defined as malignant; 5 or less was considered benign.

Statistical Analysis

The difference in mean ADC values between IDC, DCIS, and benign lesions were analyzed. We compared the ADC values on DWI and BI-RADS of DCE-MRI with the histologic grades of breast cancer according to the histologic diagnosis of the breast lesions. The accuracy of DCE-MRI, the DWI-T2WI set, and combined assessment of DCE and DWI-T2WI of the breast lesions was compared. The area under the receiver operating characteristic (ROC) curve (Az) was calculated for each imaging set and fitted to each reader's confidence scoring, determining the diagnostic accuracy. The total number of cases represented the results from the combined data of the two readers, which were used to calculate the composite ROC curve and the mean Az value. The Az values for each reader, using the two methods and the combined data, were compared using the nonparametric method described by Hanley and McNeil and the previously mentioned computer software. Statistical analyses were performed with SPSS 20.0 software (IBM SPSS Statistics for Windows, IBM Corp., Armonk, NY). The chi-square test and one-way analysis of variance were performed and P values $<.05$ were considered statistically significant.

RESULTS

Of the 169 breast lesions, 121 (71.6%) were malignant, including 88 IDC, 24 DCIS, 5 invasive lobular carcinoma, and 4 mucinous carcinoma. The pathologic results of breast lesions are summarized in Table 3. The mean tumor size was 1.2 cm (range, 0.7–4.5 cm). In DCE-MRI, the circumscribed masses consisted of 25 benign and 31 malignant lesions (1 DCIS, 26 IDC, 4 mucinous carcinoma). The non-circumscribed masses consisted of 14 benign and 65 malignant lesions (1 DCIS, 62 IDC, 2 lobular carcinoma). Non-mass enhancement revealed 9 benign lesions and 25 malignancies (22 DCIS, 3 lobular carcinoma). Only 53.7% of malignant lesions had a kinetic

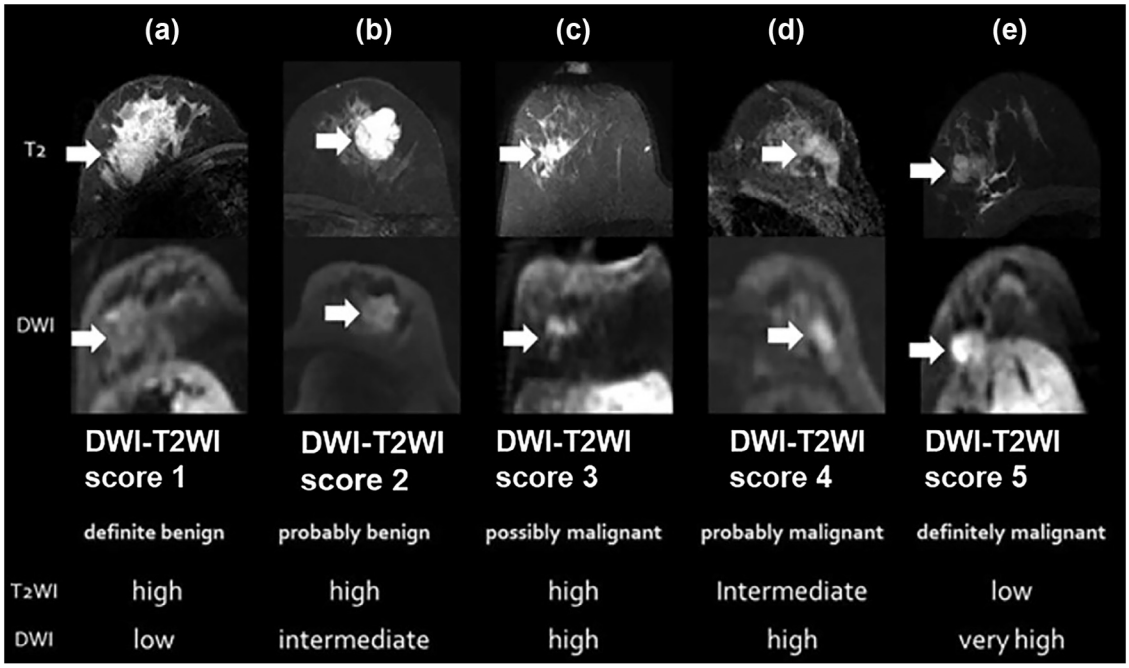

Figure 1. Examples of breast lesions for reader diffusion-weighted imaging and T2-weighted imaging (DWI-T2WI) scores used for lesion characterization. **(a)** DWI-T2WI score 1 (definitely benign) showed high signal intensity (SI) on T2WI and low SI on DWI; **(b)** DWI-T2WI score 2 (probably benign) showed high SI on T2WI and intermediate SI on DWI; **(c)** DWI-T2WI score 3 (possibly malignant) showed high SI on T2WI and high SI on DWI; **(d)** DWI-T2WI score 4 (probably malignant) showed intermediate SI on T2WI and high SI on DWI; and **(e)** DWI-T2WI score 5 (definitely malignant) showed low SI on T2WI and very high SI on DWI.

TABLE 3. Pathologic Result of Breast Lesions

Benign (n = 48)	Malignancy (n = 121)
6 Fibroadenoma	88 IDC
12 Fibrocystic change	24 DCIS
3 Columnar-cell changes	5 Invasive lobular carcinoma
4 Phyllodes tumor	4 Mucinous carcinoma
12 Intraductal papilloma	
1 Tuberculous granulomatosis	
1 Diabetes mellitus mastopathy	
2 Sclerosing adenosis	
7 Atypical ductal hyperplasia	

IDC, invasive ductal carcinoma; DCIS, ductal carcinoma in situ.

curve of 3 (65/121), and only 64.5% of benign lesions had a kinetic curve of 1 (24/48). A total of 42.9% of malignant lesions (52/121) and 37.5% of benign lesions (18/48) had a kinetic curve of 2. According to the BI-RADS, the overall sensitivity, specificity, and positive predictive value (PPV) were 95.9%, 45.8%, and 81.7%, respectively. Of benign lesions, 45.8% (22/48) were misclassified as BI-RADS 4. The histopathologic results of the false-positive lesions were phyllodes tumor (4/5), intraductal papilloma (IDP) (7/10), fibrocystic change (5/11), atypical ductal hyperplasia (ADH) (4/7), sclerosing adenosis (1/2), and tuberculosis (1/1). Five malignant lesions (5/121 [4%]) were misclassified as BI-RADS 3 (4 DCIS, 1 mucinous carcinoma). The correlation of DWI-T2WI scores with histology of the lesions and comparison of sensitivity, specificity, PPV, and area under the ROC curve of DCE-MRI, DWI-T2WI set, and combined assessment of DCE and DWI-T2WI are summarized in Table 4 and Table 5. The characterization accuracies of DWI-T2WI set and combined assessment of MRI were significantly higher than that of the DCE-MRI, according to the ROC curve as seen in Figure 2. The mean Az values were 0.747 (DCE-MRI), 0.847 (DWI-T2WI set), and 0.896 (combined assessment of MRI) ($P < .05$). When an ADC value of 1.19×10^{-3} mm^2/s was used as the cutoff value for discriminating malignant lesions from benign lesions, the specificity and sensitivity were 85.3% and 87.3%, respectively. In the DWI-T2WI set, the histopathologic results of the false-negative lesions were DCIS (12/24), IDC grade 1 (5/11), mucinous carcinoma (3/4), and invasive lobular carcinoma (4/5). The histopathologic results of the false-positive lesions were ADH (4/7), IDP (1/10), and tuberculosis (1/1). A total of 13 DCIS lesions demonstrated non-mass enhancement with a kinetic curve of 2 on DCE-MRI and a DWI-T2WI score of 2, with slightly high ADC values (>1.29×10^{-3}mm^2/s). Phyllodes tumor demonstrated circumscribed heterogeneously enhancing mass with kinetic curve 2 in DCE-MRI (BI-RADS 4). However, in DWI-T2WI set, benign phyllodes tumor showed a high SI on T2WI and an intermediate SI with high ADC value (1.4×10^{-3} mm^2/s), DWI-T2WI score of 2, considered probably benign (Fig 3). In DWI-T2WI set, high–grade-invasive carcinoma demonstrated intermediate or low SI on T2WI and markedly high SI on DWI with low ADC value (less than 0.75×10^{-3} mm^2/s), DWI-T2WI score of 5 (Fig 4). The mean

TABLE 4. Correlation of DWI-T2WI Scores with Histology of the Lesions

DWI-T2WI Score	Benign (n = 48)	Malignant (n = 121)	Number of Lesions (n = 169)	*P* Value*
Score 1: definitely benign	9 (18.7)	0 (0)	9 (5.3)	.00
Score 2: probably benign	33 (6.9)	22 (18.2)	55 (32.5)	
Score 3: possibly malignant	2 (4.2)	23 (19.0)	25 (14.8)	
Score 4: probably malignant	3 (6.3)	37 (30.6)	40 (23.7)	
Score 5: definitely malignant	1 (2.1)	39 (32.2)	40 (23.7)	

DWI-T2WI, diffusion-weighted imaging and T2-weighted imaging.
* By chi-square test.

TABLE 5. Comparison of Sensitivity, Specificity, PPV, and AUC of DCE-MRI, DWI-T2WI Set, and Combined Assessment of DCE and DWI-T2WI

Results	DCE-MRI Set	DWI-T2WI Set	Combined Assessment of DCE and DWI-T2WI
Sensitivity (%)	95.9	81.8	83.5
Specificity (%)	45.8	87.5	91.7
PPV (%)	81.7	94.2	96.2
AUC (95% CI)	0.854 (0.797–0.911)	0.876 (0.818–0.934)	0.922 (0.878–0.965)

AUC, area under the receiver operating characteristic curve; CI, confidence interval; DCE-MRI, dynamic contrast-enhanced magnetic resonance imaging; DWI-T2WI, diffusion-weighted imaging and T2-weighted imaging; PPV, positive predictive value.

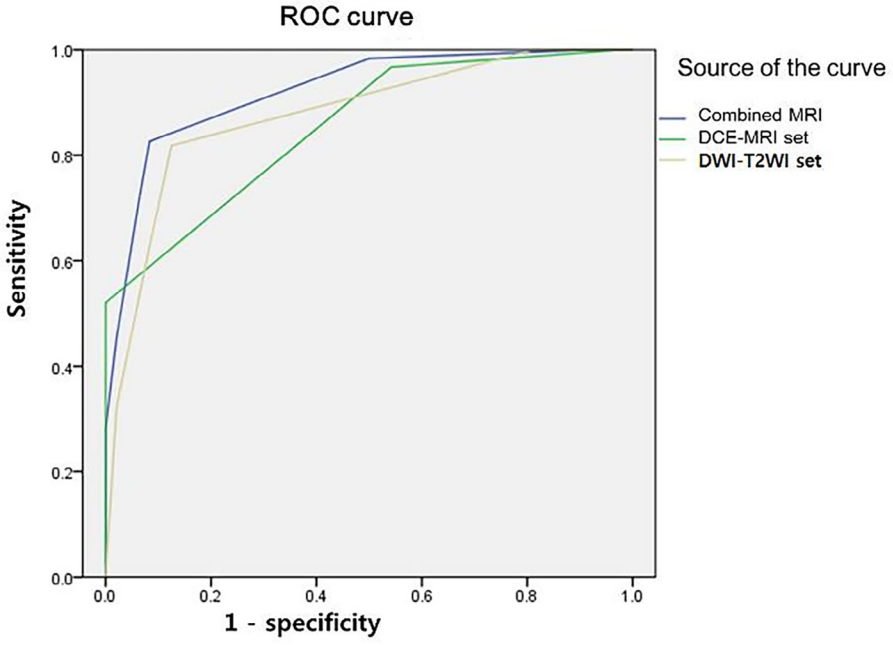

Figure 2. Composite receiver operating characteristic (ROC) curves. The ROC curves show reader confidence in the characterization of malignant breast tumors using the diffusion-weighted imaging and T2-weighted imaging (DWI-T2WI) set, the dynamic contrast-enhanced magnetic resonance imaging (DCE-MRI) set, and combined assessment of MRI. The mean area under the ROC (Az) values are 0.922 (combined assessment of MRI), 0.876 (DWI-T2WI set), and 0.854 (DCE-MRI set) ($P < .05$). FPF = false-positive fraction; TPF = true positive fraction.

ADC value was the highest in mucinous cancer and the lowest in IDC high histologic grade (Table 6, Fig 5), with a statistically significant difference ($P = .00$) between subtypes. We compared the ADC values of IDC, DCIS, and benign lesions. The mean ADC value was $1.36 \pm 0.22 \times 10^{-3}$ mm^2/s for a benign lesion and $0.96 \pm 0.20 \times 10^{-3}$ mm^2/s for a malignant lesion; this difference was statistically significant ($P < .05$). The diagram in Figure 6 showed the mean ADC of IDC and DCIS was significantly lower than that of a benign lesion ($P = .00$). Also, the mean ADC of DCIS was statistically higher than that of IDC ($P = .00$). However, the mean ADC value was not statistically different between tumor-size subgroups ($P > .05$).

DISCUSSION

Our study shows a higher sensitivity of the DCE-MRI than both the DWI-T2WI set and combined assessment of DCE and DWI-T2WI for breast lesions (95.9% vs 81.8% and 83.5%),

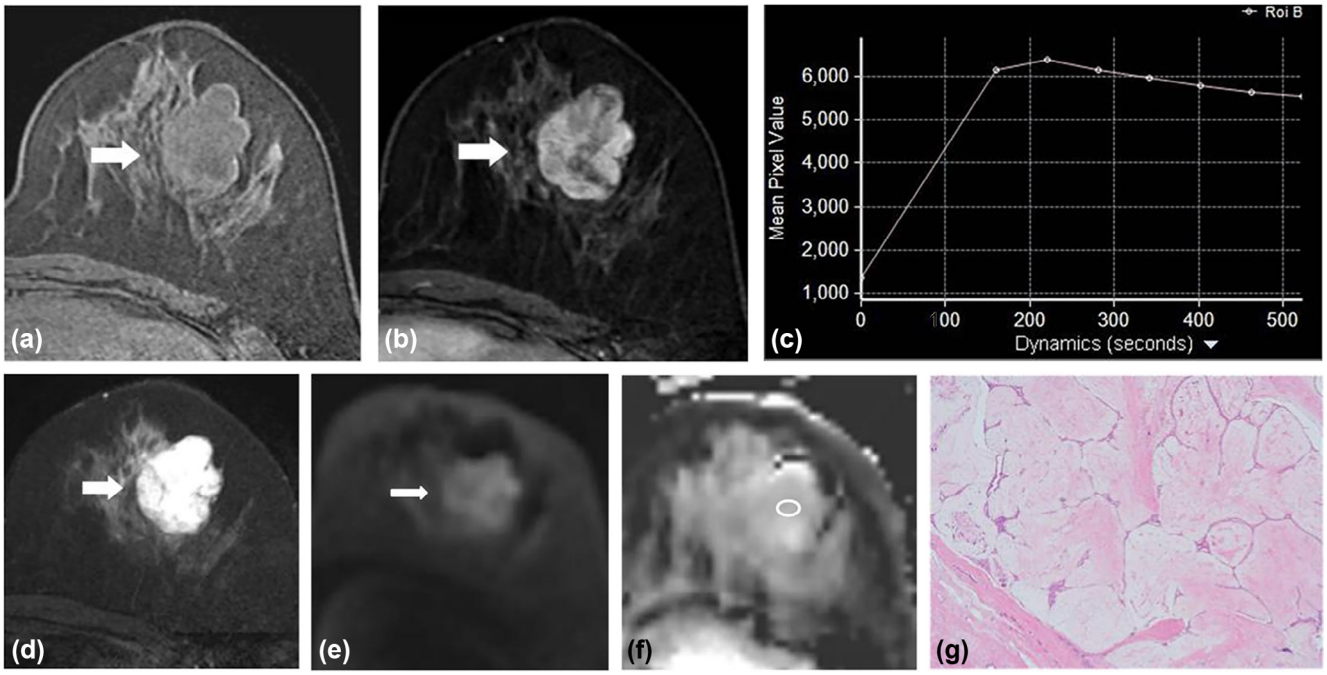

Figure 3. A 33-year-old woman with a palpable mass in the left breast. Pathology confirmed a benign phyllodes tumor. **(a)** Precontrast axial T1-weighted fast field echo (FFE), **(b)** postcontrast T1-weighted FFE (3 minutes after gadobutrol injection); **(c)** kinetic curve; **(d)** T2-weighted turbo-spin echo (TSE) with fat suppression (T2 SPAIR); **(e)** axial diffusion-weighted imaging (DWI) single-shot echo-planar image (EPI); and **(f)** focus of restricted diffusion on the apparent diffusion coefficient (ADC) map (b value, 1000 s/mm^2). The dynamic contrast-enhanced magnetic resonance imaging (DCE-MRI) set **(a, b, c)** shows a 2.5-cm circumscribed, heterogeneously enhancing, oval mass in the upper mid portion of the left breast with a kinetic curve of 2 (BI-RADS C4). The diffusion-weighted imaging and T2-weighted imaging (DWI-T2WI) set **(d, e, f)** shows a high signal intensity in the left breast mass on T2WI and an intermediate signal intensity (ADC value, 1.4×10^{-3} mm^2/s). Therefore, it was scored as DWI-T2WI 2, considered probably benign. The value of combined assessment of DCE and DWI-T2WI was 6 (sum of BI-RADS C4 and DWI-T2WI score 2), considered benign. Histopathology **(g)** showed leaf-like projections of stroma covered by epithelium, consistent with benign phyllodes tumor (hematoxylin and eosin [H&E] stain; × 40). DWI-T2WI sets with ADC values were more useful to diagnose benign tumor than the DCE-MRI set. BI-RADS, Breast Imaging-Reporting and Data System; SPAIR, spectral attenuated inversion recovery.

but the specificity and PPV of DWI-T2WI set and combined assessment of DCE and DWI-T2WI (specificity, 87.5% and 91.7%; PPV, 94.3% and 96.2%, respectively) were significantly higher than those of the DCE-MRI (specificity, 45.8%; PPV, 81.7%).

The ADC values obtained with the use of a high b value are more effective for differentiating malignant from benign tumors. Therefore, we used high b values in this study. Using a b value of 1000 s/m^2, the mean ADC value of the malignant lesions was $0.91 \pm 0.22 \times 10^{-3}$ mm^2/s and that of benign lesions was $1.35 \pm 0.23 \times 10^{-3}$ mm^2/s. These results are similar to other studies where b values of 1000 s/m^2 were used; the mean ADC value of malignancy was $0.97 \pm 0.20 \times 10^{-3}$ mm^2/s according to Guo et al. (16) and $1.09 \pm 0.27 \times 10^{-3}$ mm^2/s according to Kim et al. (17).

The characterization accuracy of the DWI set and combined MRI is significantly higher than with the DCE-MRI set, as seen by our ROC curve. The mean Az values of combined MRI (0.922) and the DWI set (0.876) are higher than that of the DCE-MRI set (0.854). The reason for this is not certain, although the phenomenon is assumed to contribute to the observed higher specificity and lower false-positive fraction in the DWI set compared with the DCE-MRI set. The need for combined interpretation of DWI and T2WI must be emphasized. The SI of breast malignancy on DWI is higher than that of T2WI (DWI-T2WI scores 3, 4, and 5), but the SI of benign breast lesions on DWI is lower than that of T2WI (DWI-T2WI scores 1 and 2). The DWI-T2WI set is better than DCE-MRI for detection and characterization of benign breast lesions. In DCE-MRI, only 53.7% of malignant lesions had a kinetic curve of 3 (65/121), and only 64.5% of benign lesions had a kinetic curve of 1 (24/48) in our study. A total of 42.9% of malignant lesions (52/121) and 37.5% of benign lesions (18/48) had a kinetic curve of 2. Analysis of the kinetic curve showed it was not a good differentiator between malignant and benign breast lesions. In Figure 3, the DCE-MRI set showed a lobulated enhancing mass with a kinetic curve of 2 (BI-RADS 4). The DWI-T2WI set showed a high SI on T2WI and an intermediate SI on DWI (DWI-T2WI score 2), considered probably benign. Histopathologic result was a benign phyllodes tumor. DWI-T2WI set with ADC value was more useful to diagnose benign tumor than the DCE-MRI set.

Papillary lesions have high cellularity and vascularization, so papillomas commonly show restricted diffusion, despite being benign lesions (2,16,18). In addition, ADH can cause diagnostic

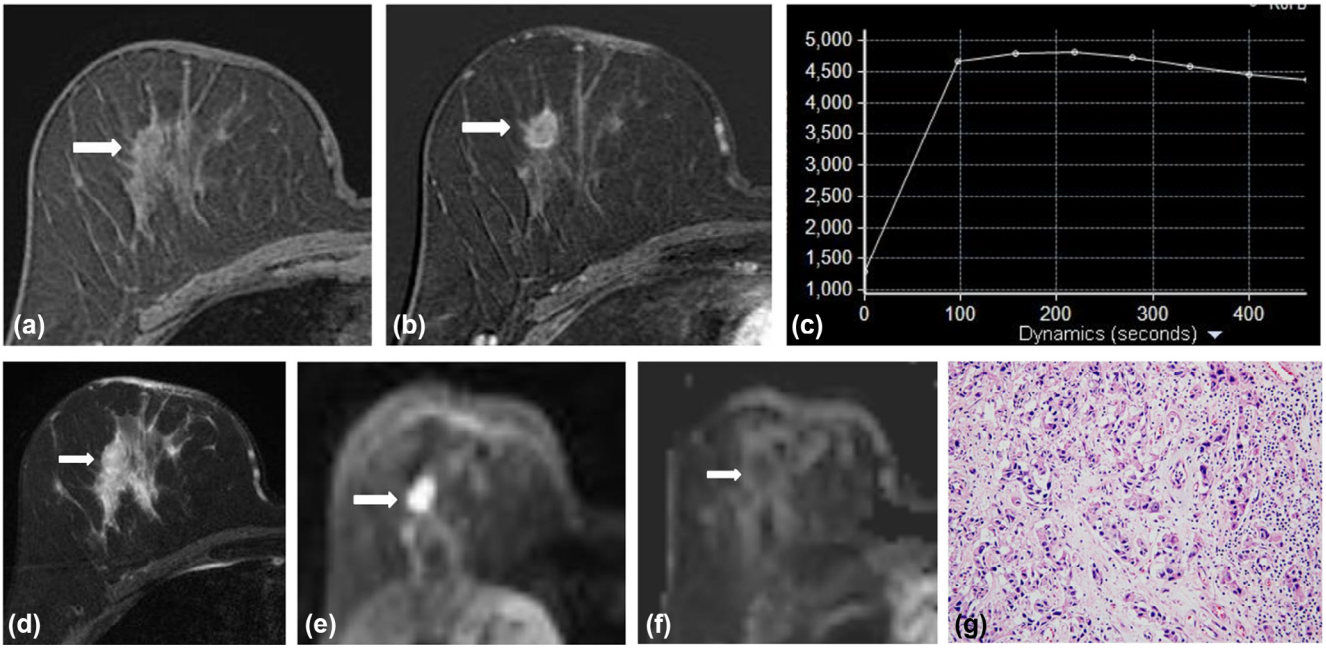

Figure 4. A 57-year-old woman with a right breast mass. Pathology demonstrated a high-grade invasive ductal carcinoma. **(a)** Precontrast axial T1-weighted FFE; **(b)** postcontrast subtraction image (by subtracting the precontrast images from the 3 minutes postcontrast images); **(c)** kinetic curve; **(d)** T2 SPAIR; **(e)** axial DWI single-shot EPI; **(f)** focus of restricted diffusion on the ADC map (b value, 1000 s/mm^2). The DCE-MRI set **(a, b, c)** shows a 1.0-cm circumscribed, round homogeneously enhancing mass in the subareolar area of the right breast with kinetic curve 2. Note, the diffuse skin thickening of the right breast (BI-RADS C4). The DWI-T2WI set **(d, e, f)** shows intermediate SI mass in the right breast on T2WI and marked high SI lesion on DWI (ADC value, 0.67×10^{-3} mm^2/s). Therefore, it was scored as DWI-T2WI 5, considered definitely malignant. The value of combined assessment of DCE-DWI-T2WI was 9 (sum of BI-RADS C4 and DWI-T2WI score 5), considered malignant. Histopathology **(g)** showed invasive ductal carcinoma with a high histologic grade. Nuclei showed marked variation in size and shape with mitoses (Bloom and Richardson grade 3; tubule formation, 3; nuclear pleomorphism, 3; mitoses, >10 HPF) (H&E stain, ×400). ADC, apparent diffusion coefficient; BI-RADS, Breast Imaging-Reporting and Data System; DCE-MRI, dynamic contrast-enhanced magnetic resonance imaging; DWI-T2WI, diffusion-weighted imaging and T2-weighted imaging; EPI, echo-planar image; FFE, fast field echo; H&E, hematoxylin and eosin; HPF, high-power field; SI, signal intensity; SPAIR, spectral attenuated inversion recovery.

TABLE 6. Correlation of ADC Values with Histopathology and Histologic Grade of Breast Lesions

	No. of Lesions (n = 169)	ADC (10^{-3} mm^2/s) (Mean ± SD)	*P* Value*
Benign	48 (28.4)	1.36 ± 0.22	.00
Malignant (DCIS + IDC)	121 (71.6)	0.96 ± 0.20	
DCIS	24 (19.8)	1.11 ± 0.13	.00
IDC	88 (72.7)	0.89 ± 0.17	
Mucinous carcinoma	4 (3.3)	1.42 ± 0.21	
Invasive lobular carcinoma	5 (4.1)	1.16 ± 0.63	
DCIS	24 (19.8)	1.11 ± 0.13	.00
IDC grade 1	11 (6.5)	1.04 ± 0.26	
IDC grade 2	43 (25.4)	0.97 ± 0.21	
IDC grade 3	43 (25.4)	0.84 ± 0.15	

ADC, apparent diffusion coefficient; ANOVA, analysis of variance; DCIS, ductal carcinoma in situ; IDC, invasive ductal carcinoma; SD, standard deviation.

* By paired *t* test or one-way ANOVA.

difficulties on both DCE-MRI and DWI due to either suspicious morphology or strong enhancement with low ADC values (2,16,18,19). The ADC values for IDP range from 0.95×10^{-3} mm^2/s to 1.50×10^{-3} mm^2/s, whereas those for ADH range from 0.90×10^{-3} mm^2/s to 1.03×10^{-3} mm^2/s.

Several studies have reported that ADC values appear to be lower in IDC than in DCIS (5,11,16,20–22). Consistent with previous studies, our study demonstrated that the mean ADC value of IDC ($0.89 \pm 0.17 \times 10^{-3}$ mm^2/s) is significantly lower than that of DCIS ($1.11 \pm 0.13 \times 10^{-3}$ mm^2/s; $P < .01$). In our study, 50% of DCIS lesions (12/24) had non-mass enhancement, no restricted diffusion, and high ADC values, causing false-negative results. The mean ADC for malignant masses with non-mass enhancement is higher than that of malignant masses. The mean ADC value of invasive lobular carcinoma showing non-mass enhancement is higher than that of IDC. A few studies have analyzed the relation between tumor grading and ADC values. Several studies have reported no significant correlation between the ADC value and the histologic grade of a tumor (17–21). Other studies have reported that the mean ADC value has a significant correlation

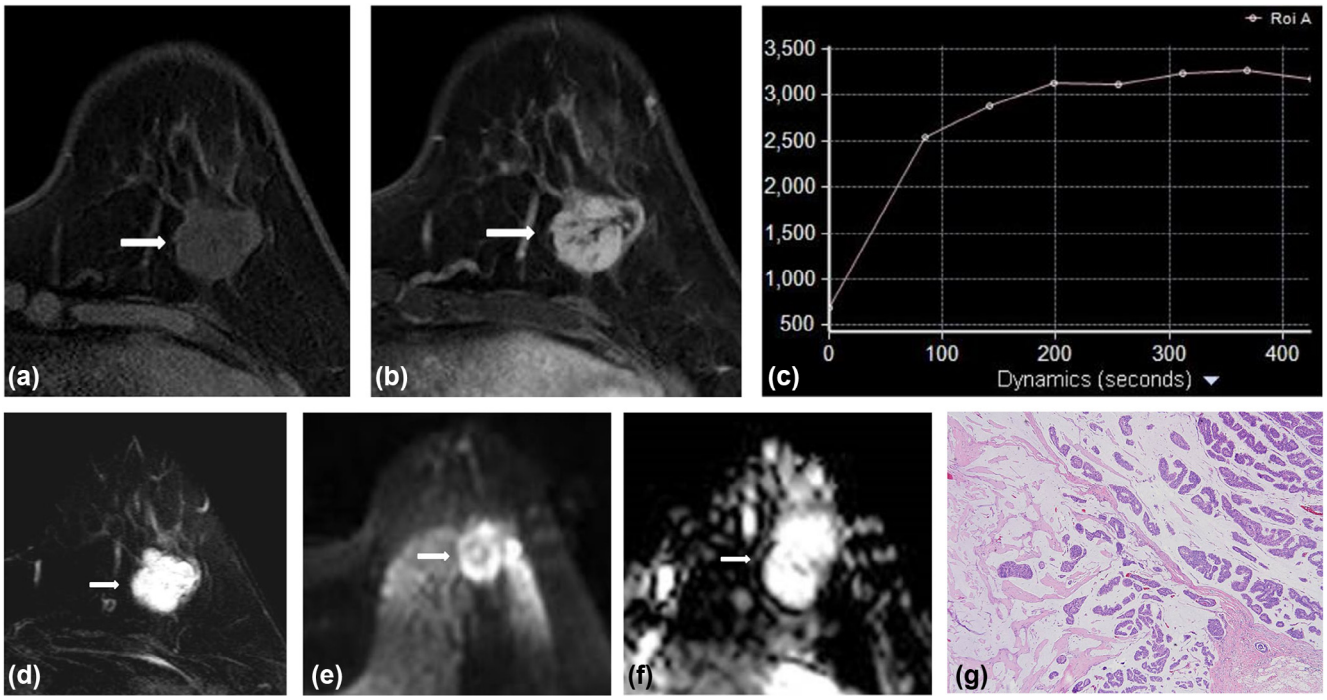

Figure 5. A 58-year-old woman with a palpable left breast mass. Pathology confirmed a mucinous carcinoma. **(a)** Precontrast axial T1-weighted FFE; **(b)** postcontrast T1-weighted FFE (3-minute postcontrast dynamic series); **(c)** kinetic curve; **(d)** T2 SPAIR; **(e)** axial DWI single-shot EPI; **(f)** focus of restricted diffusion on the ADC map (b value, 1000 s/mm^2). The DCE-MRI set **(a, b, c)** showed a circumscribed heterogeneous enhancing, oval mass in the upper outer quadrant of the left breast, with a kinetic curve of 2 (BI-RADS 4). The DWI-T2WI set **(d, e, f)** showed a strong, high SI in the left breast mass on T2WI and a low SI on DWI, with a high ADC value (1.45×10^{-3} mm^2/s). Therefore, it was scored as DWI-T2WI score 2, considered probably benign. The value of combined assessment of DCE and DWI-T2WI was 6 (sum of BI-RADS C4 and DWI-T2WI score 2), considered benign. Histopathology **(g)** showed abundant mucin with tumor cells from mucinous carcinoma (H&E stain, ×100). Because of the high ADC value of mucinous carcinoma, we misdiagnosed this tumor by both the DWI-T2WI set and combined assessment of MRI. ADC, apparent diffusion coefficient; BI-RADS, Breast Imaging-Reporting and Data System; DCE-MRI, dynamic contrast-enhanced magnetic resonance imaging; DWI-T2WI, diffusion-weighted imaging and T2-weighted imaging; EPI, echo-planar image; FFE, fast field echo; H&E, hematoxylin and eosin; HPF, high-power field; SI, signal intensity; MRI, magnetic resonance imaging; SPAIR, spectral attenuated inversion recovery.

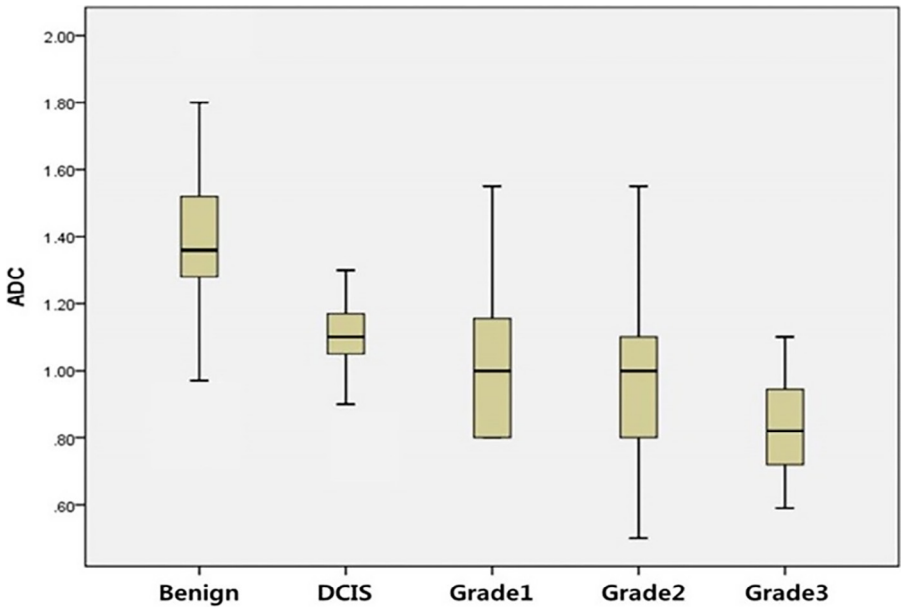

Figure 6. Diagram of ADC values for benign and malignant lesions. Box plots show the median and interquartile ranges (25th and 75th percentiles) of the ADC value in benign lesion, DCIS, invasive ductal carcinoma grades 1, 2, and 3 lesions. The mean ADC value was 1.36 ± 0.22^{-3} mm^2/s for benign lesions and 0.96 ± 0.20^{-3} mm^2/s for malignant lesions; this difference was statistically significant. The mean ADC of ductal carcinoma in situ (1.11 ± 0.13^{-3} mm^2/s) was statistically higher than that of invasive ductal carcinoma (0.89 ± 0.17^{-3} mm^2/s) ($P < .05$). The mean ADC value was significantly associated with histologic grade ($P < .05$), which is the lowest in grade 3 (0.84 ± 0.15^{-3} mm^2/s). ADC, apparent diffusion coefficient; DCIS, ductal carcinoma in situ.

with the histologic grade (22–26). In our study, histologic grading in IDC had a significant correlation with the ADC value. The mean ADC value was $1.04 \pm 0.26 \times 10^{-3}$ mm^2/s in low grade tumors, $0.97 \pm 0.21 \times 10^{-3}$ mm^2/s in intermediate grade tumors, and $0.84 \pm 0.15 \times 10^{-3}$ mm^2/s in high grade tumors, showing that the ADC value is the lowest for high grade tumor ($P = .02$). Rim enhancement was correlated with a higher histologic grade. However, the mean ADC value was not statistically different between tumor-size subgroups. Several studies have reported a correlation of MRI features and ADC values with pathologic prognostic factors. A spiculated margin is a significant predictor of lower histologic grade and a lower expression of Ki-67 (27). Rim enhancement is a significant predictor of higher histologic grade, negative expression of estrogen receptor and progesterone receptor, and a larger tumor size. A low ADC value is correlated with positive expression of estrogen receptor and progesterone receptor, and an increased Ki-67 index (17,19,23,24). In our current study, rim enhancement was correlated with a higher histologic grade, but we did not include the correlation between the ADC value and immunochemical prognostic factors. We plan to extend our study to include this correlation in the future.

Mucinous carcinomas in our study had much higher mean ADC values than either of the other types of breast cancers or the benign tumors. This is consistent with the results of previous studies (11,28). Mucinous carcinomas contain mucin pools; T2 SI and the enhancement rate of these tumors depend on the amount of mucin present. Although the cause of high ADC values obtained from these tumors is not clear, it may be related to their mucin component and low cellularity. In our study, the mean ADC of mucinous carcinoma ($1.42 \pm 0.21 \times 10^{-3}$ mm^2/s) is statistically higher than that of both benign lesions ($1.36 \pm 0.22 \times 10^{-3}$ mm^2/s) and malignant lesions ($0.96 \pm 0.20 \times 10^{-3}$ mm^2/s) (Fig 5).

The main limitation of our study is that the DWI-T2WI score we used must be further validated with an accepted clinical parameter for detecting clinical outcomes for breast lesions. We are in the process of establishing a registry for all of our patients that includes MRI and DWI. Understanding the additive value of combining DWI and T2WI with ADC values for breast disease provided an increased accuracy over DCE-MRI for differentiation between benign and malignant lesions. However, it will have to be further evaluated. The second limitation is that our study evaluated a small number of tumor samples. The number of breast lesions was too small to make definitive comparisons between malignant and benign lesions. We usually perform MRI and DWI for the purpose of preoperative evaluation of suspected breast cancer. Therefore, we could not obtain a sufficient number of benign lesions, mucinous carcinomas, lobular carcinomas, and medullary carcinomas. The third limitation is that our study evaluated tumor sizes ranging from 7 mm to 45 mm. We used a small ROI, in two different places, to obtain the ADC value measurements. This is not able to completely reflect the characteristics of large tumors. Finally, the images were interpreted by two radiologists in consensus, but interobserver variability could not be determined.

In conclusion, the combination of DWI-T2WI provides increased accuracy for differentiation between benign and malignant lesions, compared with DCE-MRI alone. A low ADC value and rim enhancement were associated with a higher histologic grade cancer. Our study suggests that there could be an additive value of combining DWI, T2WI, and ADC values for the assessment of differentiation between benign and malignant lesions. Also, the addition of DWI with T2WI to DCE-MRI may play a role as a noninvasive method to help to identify the histologic grade of breast cancer. Nevertheless, our findings should be considered preliminary results and a large multicenter trial is needed for further investigation.

REFERENCES

1. Wenkel E, Geppert C, Schulz-Wendtland R, et al. Diffusion weighted imaging in breast MRI: comparison of two different pulse sequences. Acad Radiol 2007; 14:1077–1083.
2. Marini C, Iacconi C, Gianelli M, et al. Quantitative diffusion-weighted MR imaging in differential diagnosis of breast lesion. Eur Radiol 2007; 17:2646–2655.
3. Hatakenenaka M, Sodea H, Yabuuchi H, et al. Apparent diffusion coefficients of breast tumors: clinical application. Magn Reson Med Sci 2008; 7:23–29.
4. Partridge SC, Mullins CD, Kurland BF, et al. Apparent diffusion coefficient values for discriminating benign and malignant breast MRI lesions: effects of lesion type and size. AJR Am J Roentgenol 2010; 194:1664–1673.
5. Rubesova E, Grell AS, De Maertelaer V, et al. Quantitative diffusion imaging in breast cancer: a clinical prospective study. J Magn Reson Imaging 2006; 24:319–324.
6. Kinoshita T, Yashiro N, Ihara N, et al. Diffusion-weighted half-Fourier single-shot turbo spin echo imaging in breast tumors: differentiation of invasive ductal carcinoma from fibroadenoma. J Comput Assist Tomogr 2002; 26:1042–1046.
7. Yoshitakawa MI, Ohsumi S, Sugata S, et al. Relation between cancer cellularity and apparent diffusion coefficient values using diffusion-weighted magnetic resonance imaging in breast cancer. Radiat Med 2008; 26:222–226.
8. Merchant TE, Thelissen GR, de Graaf PW, et al. Application of a mixed imaging sequence for MR imaging characterization of human breast disease. Acta Radiol 1993; 34:356–361.
9. Sugahara T, Korogi Y, Kochi M, et al. Usefulness of diffusion-weighted MRI with echo-planar technique in the evaluation of cellularity in gliomas. J MagnReson Imaging 1999; 9:53–60.
10. Gauvain KM, McKimstry RC, Mukherjee P, et al. Evaluating pediatric brain tumor cellularity with diffusion-tensor imaging. AJR Am J Roentgenol 2001; 177:449–454.
11. Kul S, Causu A, Alhan E, et al. Contribution of diffusion-weighted imaging to dynamic contrast-enhanced MRI in the characterization of breast tumors. AJR Am J Roentgenol 2011; 196:210–217.
12. Bakrya MAH, Sultana AA, Tokhya NAE, et al. Role of diffusion weighted imaging and dynamic contrast enhanced magnetic resonance imaging in breast tumors. Egypt J Radiol Nucl Med 2015; 46:791–804.
13. Maltez de Almeida JR, Gomes AB, Barros TP, et al. Subcategorization of suspicious breast lesions (BI-RADS category 4) according to MRI criteria: role of dynamic contrast-enhanced and diffusion-weighted imaging. AJR Am J Roentgenol 2015; 205:222–231.
14. Bansal R, Shah V, Aggarwal B. Qualitative and quantitative diffusion-weighted imaging of the breast at 3T—a useful adjunct to contrast-enhanced MRI in characterization of breast lesions. Indian J Radiol Imaging 2015; 25:397–403.
15. Zhang L, Tang M, Min Z, et al. Accuracy of combined dynamic contrast-enhanced magnetic resonance imaging and diffusion-weighted imaging for breast cancer detection: a meta-analysis. Acta Radiol 2016; 57:651–660.

16. Guo Y, Cai YQ, Cai ZL, et al. Differentiation of clinically benign and malignant breast lesions using diffusion-weighted imaging. J Magn Reson Imaging 2002; 16:172–178.
17. Kim SH, Cha ES, Kim HS, et al. Diffusion-weighted imaging of breast cancer: correlation of the apparent diffusion coefficient value with prognostic factors. J Magn Reson Imaging 2009; 30:615–620.
18. Woodhams R, Matsunaga K, Kan S, et al. ADC mapping of benign and malignant breast tumors. Magn Reson Med Sci 2005; 4:35–42.
19. Jeh SK, Kim SH, Kim HS, et al. Correlation of the apparent diffusion coefficient value and dynamic magnetic resonance imaging findings with prognostic factors in invasive ductal carcinoma. J Magn Reson Imaging 2011; 33:102–109.
20. Choi SY, Chang YW, Park HJ, et al. Correlation of the apparent diffusion coefficiency values on diffusion-weighted imaging with prognostic factors for breast cancer. Br J Radiol 2012; 85:474–479.
21. Yoshikawa MI, Ohsumi S, Sugata S, et al. Relation between cancer cellularity and apparent diffusion coefficient values using diffusion weighted magnetic resonance imaging in breast cancer. Radiat Med 2008; 26:222–226.
22. Park SH, Choi HY, Hahn SY. Correlation between apparent diffusion coefficient values of invasive ductal carcinoma and pathologic factors on diffusion-weighted MRI at 3.0 Tesla. J Magn Reson Imaging 2015; 41:175–182.
23. Razek AA, Gaballa G, Denewer A, et al. Invasive ductal carcinoma: correlation of apparent diffusion coefficient value with pathological prognostic factors. NMR Biomed 2010; 23:619–623.
24. Kitajima K, Yamano T, Fukushima K, et al. Correlation of the SUVmax of FDG-PET and ADC values of diffusion-weighted MR imaging with pathologic prognostic factors in breast carcinoma. Eur J Radiol 2016; 85:943–949.
25. Yırgın IK, Arslan G, Öztürk E, et al. Diffusion weighted MR imaging of breast and correlation of prognostic factors in breast cancer. Balkan Med J 2016; 33:301–307.
26. Yuen S, Uematsu T, Kasami M, et al. Breast carcinomas with strong high-signal intensity on T2-weighted MR images: pathological characteristics and differential diagnosis. J Magn Reson Imaging 2007; 25:502–510.
27. Lee SH, Cho N, Kim SJ, et al. Correlation between high resolution dynamic MR features and prognostic factors in breast cancer. Korean J Radiol 2008; 9:10–18.
28. Woodhams R, Kakita S, Hata H, et al. Diffusion-weighted imaging of mucinous carcinoma of the breast: evaluation of apparent diffusion coefficient and signal intensity in correlation with histologic findings. AJR Am J Roentgenol 2009; 193:260–266.